

2-D scalar wave extrapolator using FE-FD operator for irregular grids

Xiang Du and John C. Bancroft. CREWES, Department of Geology and Geophysics. University of Calgary

2005 CSEG National Convention



Introduction

2D scalar wave extrapolator using FE-FD operator for irregular grids are presented. Since these involve semi-discretization by the finite element method (FEM) in the depth direction with the linear element, spatially irregular grids can be used to extrapolate wavefield in modeling and reverse-time migration. The mesh can be made locally thin to better represent structural complexity and lower velocity zones, which are treated by a fine grid, while the remaining parts of the models are represented by a coarse grid with equal accuracy. No interpolation is needed between the fine and coarse parts due to the rectangular grid cells. The accuracy of the proposed technique has been tested with a comparison to an analytical solution. The effectiveness of the method is verified by its application to a thin-layer model. At the same time, its efficiency is shown through an oblique interface with a variable velocity media.

Principle

As for FE-FD operator, it has been clearly addressed by Du and Bancroft (2004). We used finite element discretization along the depth direction and the FD method in the spatial domain to solve partial differential equations. In previous work, we tested the effect of the new method on a regular mesh. Since the FEM discretization along the depth direction is applied, the irregular grid computation along the depth direction will be adopted. As a result, oversampling of large high-velocity areas, typical for fine regular grids, is avoided in this way; it also offers the possibility of a more rational discretization to make the mesh locally thin to better represent structural complexity and low velocity zone. The following is the brief description about the principle used for irregular grids. Consider the hyperbolic model problem, with the 2-D scalar wave equation:

$$\frac{\partial^2 u}{\partial x^2} + \frac{\partial^2 u}{\partial z^2} = \frac{1}{a^2(x, z)} \frac{\partial^2 u}{\partial t^2}, \quad \text{in } \Omega, \quad (1)$$

where $u(x, z, t)$ denotes the wave displacement in the horizontal coordinate x , vertical coordinate z (where the z axis points downward) and time t , respectively, and $a(x, z)$ is the medium velocity.

Semi-discretizing the vertical coordinate (z) in the region of $[0, Z]$, one constructs a finite element function space as

$$u_h(x, z, t) = \sum_{i=1}^N u_i(t, x) N_i(z), \quad (2a)$$

and

$$\frac{\partial}{\partial z} u_h(x, z, t) = \sum_{i=1}^N u_i(t, x) \frac{d}{dz} N_i(z) = \sum_{i=1}^N u_i(t, x) B_i(z), \quad (2b)$$

where N is the nodal number. According to the Galerkin method (Lu and Guan, 1987), one can write the semi-discretized PDEs as:

$$M \frac{\partial^2 u}{\partial t^2} + Ku = H \frac{\partial^2 u}{\partial x^2} \quad (3a)$$

where

$$M = \sum_{n=1}^{N_e} M_e, \quad K = \sum_{n=1}^{N_e} K_e, \quad H = \sum_{n=1}^{N_e} H_e, \quad (3b)$$

$$M_e = \int_e \frac{1}{a(x, z)} N^T N dz, \quad K_e = \int_e B^T B dz, \quad H_e = \int_e N^T N dz. \quad (3c)$$

The discretization along the z direction by the FEM can be seen from Figure 1. From it, we can design the spacing interval according to the complexity of our research model.

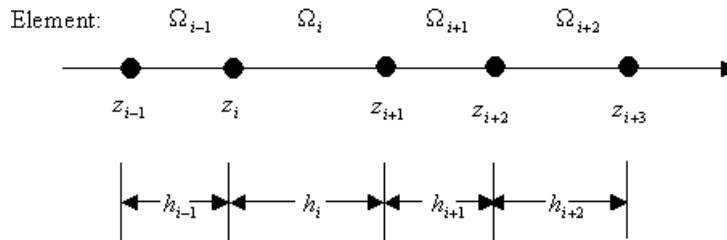


FIG 1. The discretization along the z direction by FEM

Numerical examples

In order to validate the FE-FD operator for irregular grids, four cases are chosen for modeling and migration. The numerical solution of using irregular grids for a half-plane problem is compared with the corresponding analytical solution. We also present an example of efficiently modeling wave propagation in a thin-layer model. For migration, an oblique interface model with variable velocities are chosen to show the computational efficiency of the irregular grids.

Case I: Comparison between the numerical solution with the irregular grids and analytical solution of the half-plane problem

Table 1 gives the physical parameters of the half-plane problem. Considering the usual rule of using at least ten points for the shortest wavelength of the source in this FD scheme, the grid interval along the depth alternately changes between 4 meter and 6 meter. The seismogram at a given point (Table 1) shows more quantitatively the accuracy of the numerical solution by comparison with the analytical solution (Figure 2). They are accurately matched except some difference in the amplitude.

Case II: Comparison between the numerical solution with regular grid and irregular grid for thin-layer model

The accuracy of the proposed FD technique has been verified for the homogeneous region shown as Case I. Now we apply it to effectively model wave propagation in a thin-layer model. Tests include both regular and irregular grid calculations. The size of the model is $1500 \text{ m} \times 1800 \text{ m}$. A thin-layer with 12 m thickness is imbedded in the model. The purpose is to see if the effects of the thin-layer with lower velocity can be observed in snapshots of the wavefield. The Ricker wavelet with 50 Hz is selected as the source centered in the horizontal direction and located 600 m below the top. The velocity of the thin layer is 2000 m/s, while the background velocity 4000 m/s, which are shown in Figure 3. The horizontal spacing is 5 m. For the regular grid calculation, the grid step of vertical spacing used is 6 m. In the irregular mesh, the thin grid is used only in the region of lower velocity, which is shown in the Figure 3, and the grid interval is 3 m. Other grid spacing along the depth direction is 7 m. So, the regular grid requires a total of 300×300 points, where the irregular one needs 300×260 points, which saves almost 24% fewer points compared to the regular case. The same time step ($\Delta t = 0.001\text{s}$) is used in both cases.

In order to show the result with irregular grids, we apply the cubic spline interpolation function to interpolate the one with regular grids. As for the thin-layer model, we focus our attention on the wavefield character when the wave propagates into the thin-layer. Figure 4 shows a wavefield snapshot at time 0.15 s. Reflections and transmissions from the thin lower-velocity layer can be seen. From Figure 4a, there is obvious frequency dispersion in the region of the thin-layer because a coarse grid is used in the area, while the continuity of the wavefield in the thin-layer is well described in Figure 4b.

Case III: Steep oblique interfaces migration with variable velocities

The model for this section is shown in Figure 5. The velocity of the model increases both laterally and with depth direction. The velocity at the top left corner is 3600 m/s, and the at the bottom right it is 4600 m/s. There are four reflection interfaces with a dip of 0° , 23° , 45° , and 70° . The seismogram is computed by the FDM module of the SU Software Kit, and is displayed in Figure 6. From it, one can see that there is much diffraction energy from the edges of the reflectors.

The parameters for reverse-time migration start with a grid interval of 10 m and increase by 0.04 m on each grid to a final interval of 20 m. The velocity increases in the spatial direction from 3600 to 4500. The regular grid with 10 m spacing requires a total of 100×100 , while the irregular grid requires only 100×85 , which saves some calculations. The grids partition is also shown in Figure 5. Figure 7 is the reverse-time migration result, which correctly migrated the poststack seismic section to the right oblique interface. Since there is truncation in the seismogram, we can still see some diffraction energy, which doesn't affect the migration result. When the grid spacing increases with 0.15m, the irregular one requires only 100×63 , which saves a lot of memory and calculations. The migration results are shown in Figure 11. From Figure 11a, we know there is obvious frequency dispersion problem, but from Figure 8, there is still a good match between the events and the real interfaces.

Conclusion

This paper presents a FE-FD operator approximation for the full acoustic wave equation which is able to handle nonuniform rectangular grids. The new scheme has achieved the same accuracy of a thin regular-grid calculation while reducing the computational cost in modeling and reverse-time migration. As numerical examples, it is encouraging that the result is accurate and effective enough for the simulation and migration of a complex wavefield. It is therefore a useful and promising numerical method. Only the linear element was applied along the depth direction, but extension to a quadratic element is straightforward, which gives a higher order accuracy. It is possible that a FE-FD scheme for the elastic case may also be designed using the same approach. At the same time, we can construct the irregular grids FD calculation for both the horizontal direction and vertical direction by a two-dimensional interpolation function.

Acknowledgements

We should sincerely express gratitude to Larry Lines, Edward S. Krebs and Chuck Ursebach for helpful discussions. We should also express thanks for sponsors of the CREWES project. Thanks the financial support from the CSEG scholarship. Thanks the CWP free software for my research.

Table 1. Half-plane parameters.

Physical parameters	
Velocity	3000 m/s
Source and Observer Position	$f_{main} = 50Hz$; source position: (250, 250); observer position: (150, 150).
Other parameters	$dx = 5m$, $dz = 4m$ (odd lines)/ $6m$ (even lines) $dt = 1.25E-3s$, grid of 300×300 points

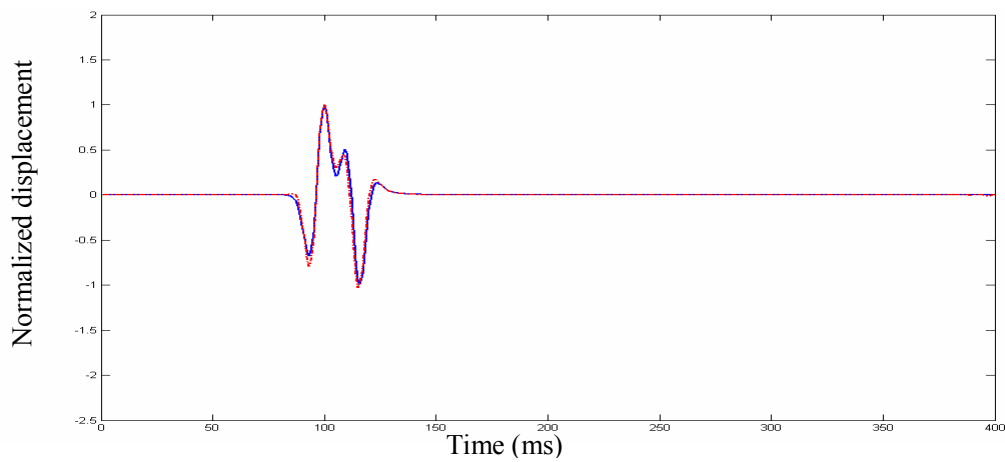


FIG 2. Seismogram at the given observer position (Table 1). The solid blue line is the analytical solution, the dashed green line is the numerical solution by FDGM with irregular grids.

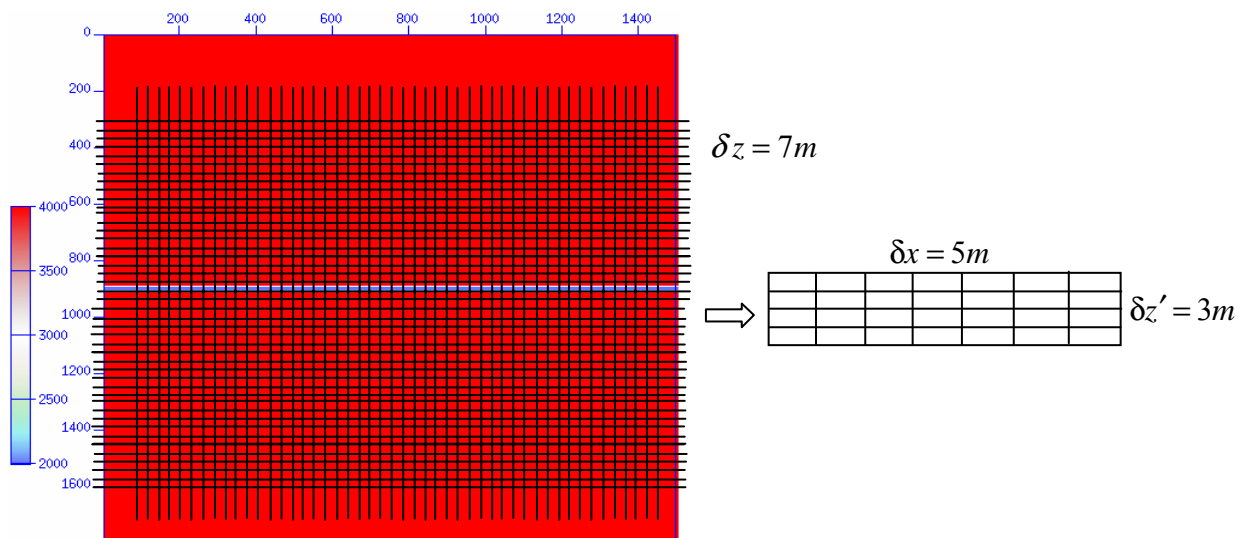


FIG 3. The velocity model and the grids partition.

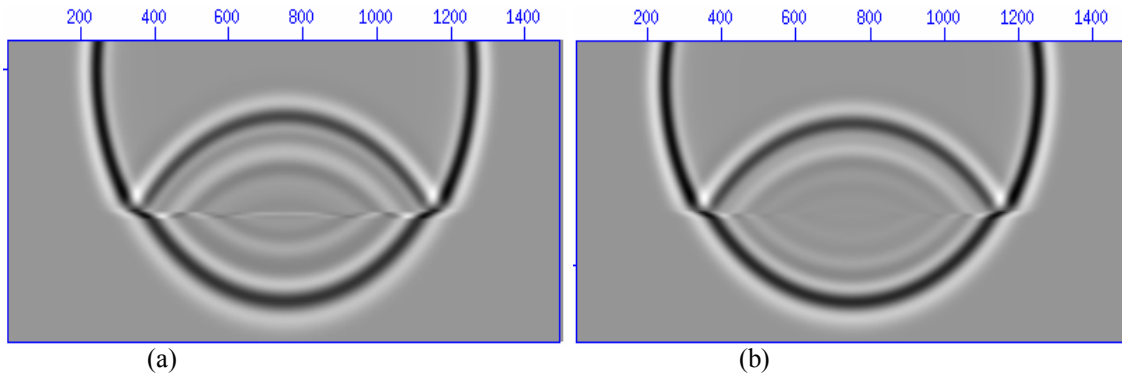


FIG 4(a) Snapshot of the wavefield ($t = 0.15$ s) with regular grids, and (b) snapshot of the wavefield ($t = 0.15$ s) with irregular grids.

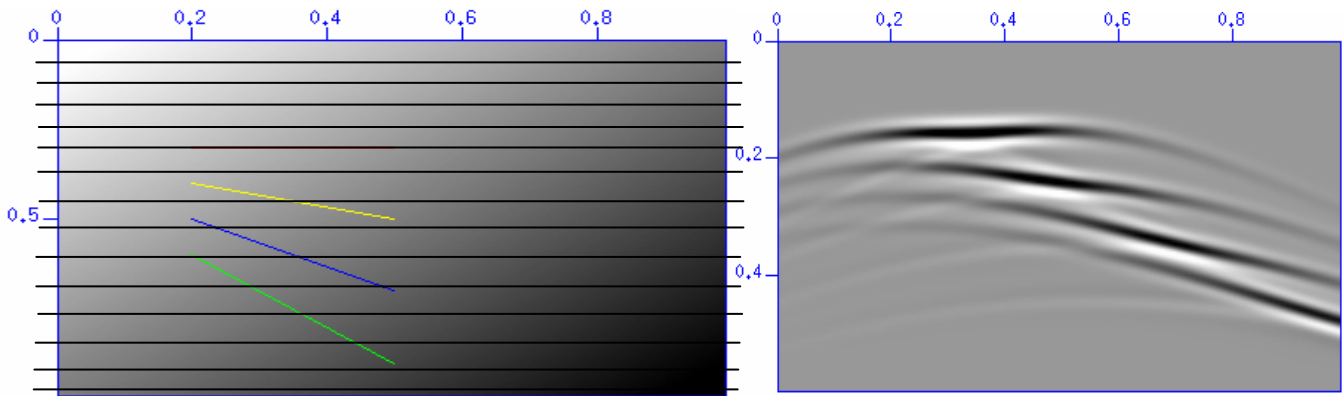


FIG 5. The steep oblique model with variable velocities. FIG 6. Seismogram generated by FDM.

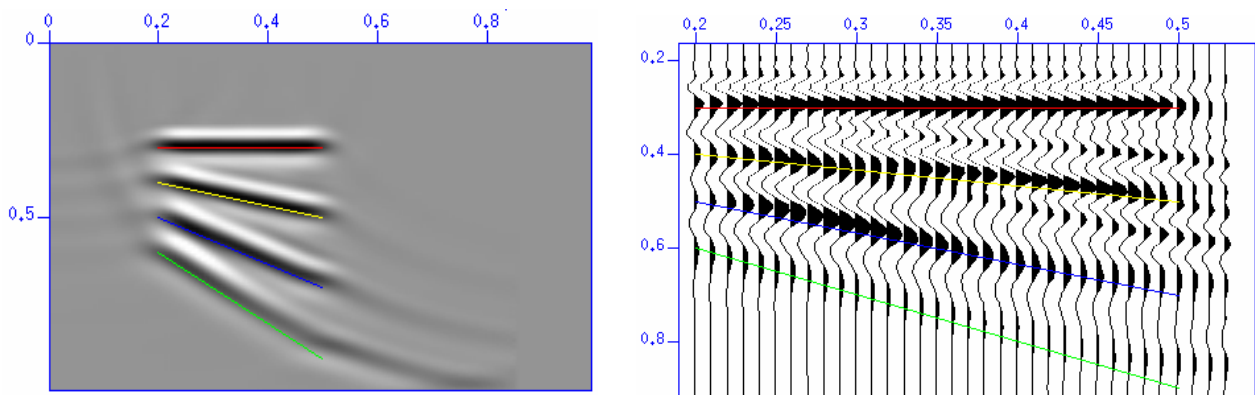


FIG 7. Reverse-time migration result(with $\Delta z=0.04$ m). FIG 8. Reverse-time migration result(with $\Delta z=0.15$ m),

References

- Du. X., and Bancroft, J., 2004, 2-D wave equation modeling and migration by a new finite difference scheme based on Galerkin method, 74th Ann. Internat. Mtg., Soc. Expl. Geophys., U.S.A
- Lu, J. and Guan, Z., 1987, Numerical method of partial differential equations (In Chinese), Beijing: Tsinghua University Press.